



Full length article

Hg⁰ oxidation and SO₃, Pb⁰, PbO, PbCl₂ and As₂O₃ adsorption by graphene-based bimetallic catalyst ((Fe,Co)@N-GN): A DFT study

Xiaoshuo Liu^{a,1}, Zhengyang Gao^{a,*,1}, Cheng Wang^{b,1}, Mingliang Zhao^a, Xunlei Ding^{c,*}, Weijie Yang^a, Zhao Ding^d

^a School of Energy and Power Engineering, North China Electric Power University, Baoding 071003, China

^b State Key Laboratory of Materials-Oriented Chemical Engineering, Nanjing University of Technology, Nanjing 21009, China

^c School of Mathematics and Physics, North China Electric Power University, Beijing 102206, China

^d Department of Mechanical, Materials and Aerospace Engineering, Illinois Institute of Technology, Chicago 60616, USA

ARTICLE INFO

Keywords:

Air pollution

Hg oxidation

Adsorption

Metal-doped graphene

ABSTRACT

As important parts of simultaneous removal of multiple pollutants in flue gas, catalytic oxidation of Hg⁰ and adsorption removal of SO₃, Pb species and As₂O₃ on the surface of (Fe,Co)@N-GN catalyst were systematically investigated in this work, using density functional theory. As a result, we found (Fe,Co)@N-GN not only showed great performance on Hg⁰ oxidation, but also exhibited outstanding removal capacity for SO₃, Pb species and As₂O₃ molecules. Besides, PDOS and EDD analysis were carried out and the result indicated that electron transfer and orbit hybridization played key roles in gas adsorption. In addition, thermodynamics analysis further evidenced (Fe,Co)@N-GN was a qualified sorbent under 550 K, and competitive analysis suggested that the adsorption order of pollution gas was determined by adsorption energy, rather than the volume fraction of corresponding gases in flue gas. We hoped this work can not only lay a foundation for theoretical investigation of Hg⁰ oxidation, but also provide an important guideline for simultaneous removal of multiple pollutants released from coal-fired power plants.

1. Introduction

Elimination of toxic gases in air has drawn increasing concern since their huge damage to environment and human's health [1]. Coal-fired power plant has widely been considered as one of the main sources of air pollution [2–4], demonstrating the abatement of poisonous gases from coal-fired power plants has become more than urgent.

Nitrogen oxides (NO [5] and NO₂ [6]), sulfur dioxides (SO₂ [7] and SO₃ [8]), and hazardous trace metals (HTMs, mainly include Hg⁰ [9–11], Pb⁰ [12], PbCl₂ [12], PbO [12], and As₂O₃ [13]) emitted from power plants have been recognized to mainly contribute to various environmental issues, including global warming, forming of photochemical smog, occurrence of acid rain, and serious health accidents via bioaccumulation [13,14], respectively, therefore becoming a hot topic in the fields of pollution control and chemical engineering. In china of 2017 year, the total amounts of stationary-source NO_x and SO₂ were up to 1.14 and 1.20 million ton respectively in the light of the data of annual development report of china power industry [15], and it was also implied that, even with complete air pollution control equipment,

the emission amounts of Hg⁰ in china can still reach 468.87 ton in 2017 [12,16]. Moreover, the total emission of As species and Pb species came up to 38.79 ton and 47.41 ton in china of 2017 year [12]. Given a little amount of these hazardous chemicals would bring great harm to human's health, it is really imperative for coal-fired power plants to avoid mass discharge of these chemicals while addressing flue gas from boilers.

In coal-fired power plants, it seemed pollution gases can be roughly removed by series of air control devices, involving selective catalytic reduction (SCR) equipment, electrostatic precipitators (ESP) device, and wet flue gas desulfurization (WFGD) system [17,18], however, current pollution-solving systems are too complex, causing huge burden to installation, operation, and maintenance of equipment [12]. In addition, it is worse that NH₃ used in traditional SCR device is a kind of dangerous gas [19], which can not only threaten human's health by hurting eyes, skins and respiratory systems [20], but also may result in serious safety accidents due to possible generation of ammonium salt which may block the heat exchangers in boilers [21–23], not to mention that almost all commercial catalysts applied in SCR reaction, such

* Corresponding authors.

E-mail addresses: gaozhyan@163.com (Z. Gao), dingxl@ncepu.edu.cn (X. Ding).

¹ These authors contributed to this work equally.

as V_2O_5 and WO_3 , were poisonous materials [24,25]. Accordingly, it is valuable and urgent to find alternative control measures with the characteristic of no-pollution, low-cost, and high-effective to replace conventional air solving methods in coal-fired power plants.

Currently, simultaneous removal of multiple pollutants using high-performance catalyst and sorbent has been considered as a promising method in pollution control released from coal-fired power plants, because this method can extremely simplify equipment systems, shorten operation process, downsize floor area, avoid toxic NH_3 injection, and lower the operation cost [12]. Simultaneous removal of exhaust pollution in flue gas can consist of two important processes. One is catalytic oxidation of NO and Hg^0 , and the other is adsorption removal of other poisonous chemicals. In detail, high-performance catalysts are applied to oxidize NO and Hg^0 to NO_2 and HgO clusters respectively, using green oxidant O_2 , and then newly produced NO_2 and HgO clusters can be easily adsorbed through WFGD together with SO_2 [14,26], using good water solubility of these molecules. As for subtle SO_3 in aerosol state, Pb^0 , PbO , $PbCl_2$ and As_2O_3 , which are difficult to be adsorbed by WFGD owing to poor water solubility, it is feasible to control them using outstanding catalyst via adsorption behavior. Therefore, in order to realize simultaneous removal of multiple pollutants in coal-fired power plants, it is a key step to find qualified material which not only has good catalytic oxidation performance, but also own compelling adsorption performance on other hazardous gases in flue gas.

Fe–Co bimetallic sites catalyst based on N-doped graphene support ((Fe,Co)@N-GN) was prepared from metal organic frameworks (MOFs) via extremely high temperature calcination exceeding 1100 K [27], so it not only held the porous structure and large specific surface area as MOFs, but also can stand the high temperature of flue gas with ease. Moreover, (Fe,Co)@N-GN has been seen as a kind of wonderful catalysts because of its perfect performance on various chemical reactions, such as oxygen reduction reaction (ORR) [28], CO catalytic oxidation [22], and NO catalytic oxidation [22]. According to precious works, the oxidation barrier of NO and CO on the surface of (Fe,Co)@N-GN are just 0.17 eV and 0.58 eV respectively [22]. Therefore, when flue gas passes through (Fe,Co)@N-GN, it is extremely likely that most NO as well as Hg^0 molecules can be converted to NO_2 and HgO , and then the products would be easily removed by WFGD, together with SO_2 . Therefore, it is an urgent issue to further investigate the oxidation barrier of Hg^0 and the adsorption behavior of SO_3 , Pb^0 , PbO , $PbCl_2$, and As_2O_3 on the surface of (Fe,Co)@N-GN to predict removal effect of these pollution chemicals via (Fe,Co)@N-GN catalyst.

2. Calculation method

Density functional theoretical calculation in this work was carried out with the software of Vienna ab initio simulation package (VASP 5.4.1) by using Perdew-Burke-Ernzerhof (PBE) method together with projector augmented wave (PAW) basis set [29–31]. The combination of PBE method and PAW potentials has been utilized successfully in plenty of works concerning adsorption and chemical reaction on the surface of metal doped graphene [25,32–34]. Considering the influence of magnetic property on accuracy of results, spin polarization was added in our calculations [35,36], and taking into account of van der Waals dispersion, DFT-D3 correction was adopted [37,38]. Consistent with our previous research [11,12,34], the model of graphene-based catalyst was set up on a $4 \times 4 \times 1$ graphene unit cell, together with a 15 Å vacuum layer in the direction over 2D graphene surface.

According to our previous test, the kinetic energy cutoff of plane-wave basis set and the Gaussian smearing were selected as 500 eV and 0.05 eV, respectively [12]. To obtain geometry structure of adsorption configurations, a $7 \times 7 \times 1$ Γ -centered k-point mesh grid was provided for structure optimization work, which has been proved to be rational and accurate by our previous investigations as well [12]. In addition, the force threshold of structure relaxation was set at the level of 0.02 eV/Å. In order to get more accurate single point energy, a

$15 \times 15 \times 1$ Γ -centered k-point mesh grid was selected to generate both electronic energy and charge information. Moreover, similar to our previous work [33], the method of climbing image nudged elastic band (CI-NEB [39,40]) was used by inserting eight images between the initial and final geometries, to locate the constructions of transition states in paths of Hg^0 oxidation.

Binding energy (E_b) is a great descriptor for testing stability of anchored metal atoms on graphene surface, and its value can be obtained through following equation [41]:

$$E_b = E_{(Fe,Co)@N-GN} - E_{sub+Co/sub+Fe} - E_{Fe/Co}$$

where $E_{(Fe,Co)@N-GN}$, E_{sub+Co} , E_{sub+Fe} , E_{Fe} , and E_{Co} means the electronic energy of (Fe,Co)@N-GN catalyst, (Fe,Co)@N-GN without iron atom, (Fe,Co)@N-GN without cobalt atom, individual iron atom, and individual cobalt atom, respectively.

To describe the adsorption strength of pollution gases toward (Fe,Co)@N-GN catalyst surface, the adsorption energy (E_{ads}) of each gas was calculated from the equation below [42]:

$$E_{ads} = E_{(Fe,Co)@N-GN+gas} - E_{(Fe,Co)@N-GN} - E_{gas}$$

where $E_{(Fe,Co)@N-GN+gas}$, $E_{(Fe,Co)@N-GN}$, and E_{gas} represent the energy of the stable adsorption system, the (Fe,Co)@N-GN catalyst, and the pollution gas molecule respectively. As defined here, more negative values of E_b/E_{ads} represent stronger adsorption strength, and if absolute value of E_{ads} exceeds 0.5 eV, the adsorption should belong to chemical adsorption [43].

3. Results and discussion

3.1. Research model of catalyst

To acquire structural, charge and magnetic information, the bond length of Fe–Co, Fe–N, Co–N and C–C at the edge of super cell were summarized, the charge of metal atom and substance were acquired, and the magnetic moment of catalyst model was provided in Table 1. In detail, the bond length of Fe–N and Co–N are the average value of three different values of Fe–N or Co–N. The bond length of C–C at graphene edge was calculated, in order to ensure the distortion of reaction center can hardly impact the boundary of catalyst model. Consequently, in the view from Table 1, it was clearly found that the bond length of Fe–N was very close to that of Co–N, which may well contribute to the similar atomic radius and the close steric hindrance effect, compared cobalt atom with iron atom. Moreover, the average C–C bond length at the edge of research model was 1.42 Å, which was same as that in pure graphene according to experimental data [44], suggesting the selection of $4 \times 4 \times 1$ super cell was suitable to avoid boundary effect, and the model we set up was rational and reasonable. Due to the weak electronegativity of iron and cobalt atom, the electron amounts are always being transferred to the substance from Fe (q_{Fe} , 0.89 e) and Co (q_{Co} , 0.61 e), suggesting the metal atoms played a role of electron donor, which showed great consistence with other contribution on metal-doped graphene [45].

Stability is a key issue in the design, preparation, and application of catalysts, while this pivotal investigation on (Fe,Co)@N-GN remains inadequate. To fill this gap, we calculated the binding energy of metal atoms on the support of catalyst. The binding energy of iron and cobalt atom anchored in graphene surface are 6.53 eV, and 6.79 eV, respectively, and these values are obviously larger than corresponding

Table 1

The key bond length (d), magnetic moment (M), and electron transfer (q) from support to metals for catalyst.

$d_{Fe-Co}/\text{Å}$	$d_{Fe-N}/\text{Å}$	$d_{Co-N}/\text{Å}$	$d_{C-C}/\text{Å}$	M/μ_B	q_{Fe}/e	q_{Co}/e	q_{sub}/e
2.19	1.97	1.93	1.42	3.45	0.89	0.61	–1.50

cohesive energy of Fe and Co metal bulks (4.28 and 4.43 eV respectively [46]), suggesting it is secure enough for dispersed Fe and Co atoms on catalyst to avoid migrating from anchored sites and forming metal clusters. This conclusion is in great agreement with the outstanding stability (Fe,Co)@N-GN catalyst exhibited in experiments [27,28].

The activity of catalyst is another important issue. Compared with pure graphene, (Fe,Co)@N-GN introduced nitrogen atom, iron atom and cobalt atom into defected graphene support. Considering large amounts of reports have revealed these modifications contribute to the activity of graphene obviously [35,47–49], it is possible for (Fe,Co)@N-GN to exhibit excited performance on pollution control. Unsaturated coordination environment of metal atom on graphene is one of the most important factors contributing to high activity [50]. In fact, after the co-doping of Fe and Co atoms, both Fe and Co atoms have only four coordination atoms, demonstrating these metal atoms having unsaturated coordination. Due to the forming of unsaturated coordination environment of Fe and Co atoms, there would existing active sites, suggesting (Fe,Co)@N-GN may own great reaction activity.

Besides, in order to deeply understand the characteristic of bimetallic catalyst, the relationship between dual active sites (Fe and Co) was talked about furthermore. Considering interatomic interaction should mainly contribute to collective impact of interatomic charge transfer and orbital hybridization, the deformation electronic density difference (DEDD) (based on previous cluster model [22] and drawn by Multiwfn software [51]) and the partial density of state (PDOS) of catalyst were pictured in Figs. 1(b) and 2, respectively. From Fig. 2, we observed that no orbital hybridization existed between Fe and Co atoms due to absent overlap of atomic *d* orbitals, demonstrating there was no covalent bond between Fe–Co dual metal active sites. In addition, in Fig. 1(b), we found the charge contour between two metal sites was relative sparse, consequently suggesting little electron exchanged and there was no fierce ionic bond interaction between metal active sites. Given both factors of atomic orbital hybridization and interatomic charge transfer, it seemed that the relation between catalytic sites was really weak, and the outstanding stability of catalyst might well credit the forming of Fe–N bond as well as Co–N bond, rather than the interaction from neighboring metal atoms. Furthermore, it was worth noted that, from Fig. 1(b), while electrons were concentrated between N atom and metal atoms, these aggregate electrons offset from bond center of Fe–N/Co–N, and tend to draw near N atoms apparently, suggesting electron transferring rather than electronic pair sharing occurred between N and metal atoms. Therefore, the strong binding energy of Fe as well as Co on substance should contribute to the ionic bond interaction of Fe–N and Co–N, and this conclusion was in great agreement with the considerable electron exchange amounts of Fe (0.89

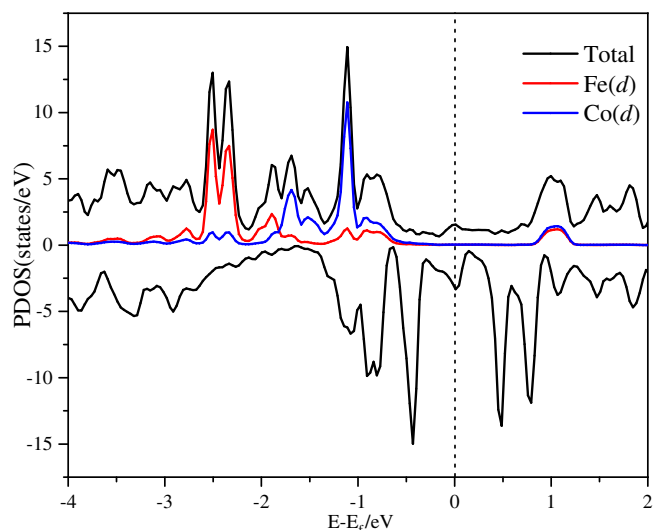


Fig. 2. The PDOS plot of (Fe,Co)/N-GN catalyst.

e) and Co (0.61 e) with N-doped graphene substance. It is worth noted that the adequate positive charge could attract small gas molecules by static induction, which may well promote the adsorption ability of sorbent for toxic chemicals.

3.2. Hg⁰ oxidation by (Fe,Co)@N-GN catalyst

3.2.1. The formation of O-Hg-O structure

Hg⁰ removal is very important in purification of flue gas from coal-fired power plants, and catalytic oxidation of Hg⁰ by O₂ has been considered to be a green and low-cost method, compared with conventional activated carbon injection (ACI) technology [52]. Therefore, the Hg⁰ oxidation by (Fe,Co)@N-GN catalyst was investigated systematically in this research, and the reaction path was provided in Figs. 3 and 4.

The adsorption order of reactant on catalyst surface is an important issue for searching reaction paths. Considering the reports of literatures, the volume fraction of O₂ (4% [14]) is far more than Hg species (0.1 ppm [22]) in flue gas. Besides, Hg⁰ was a kind of inert molecule due to its full occupied 5*d*-orbital and 6*s*-orbital, so the adsorption energy of Hg⁰ should be lower than that of O₂. Therefore, taking both factors of the volume fraction and adsorption capacity of O₂ and Hg⁰, it is nature for us to speculate that O₂ adsorption is the first step for Hg⁰ oxidation.

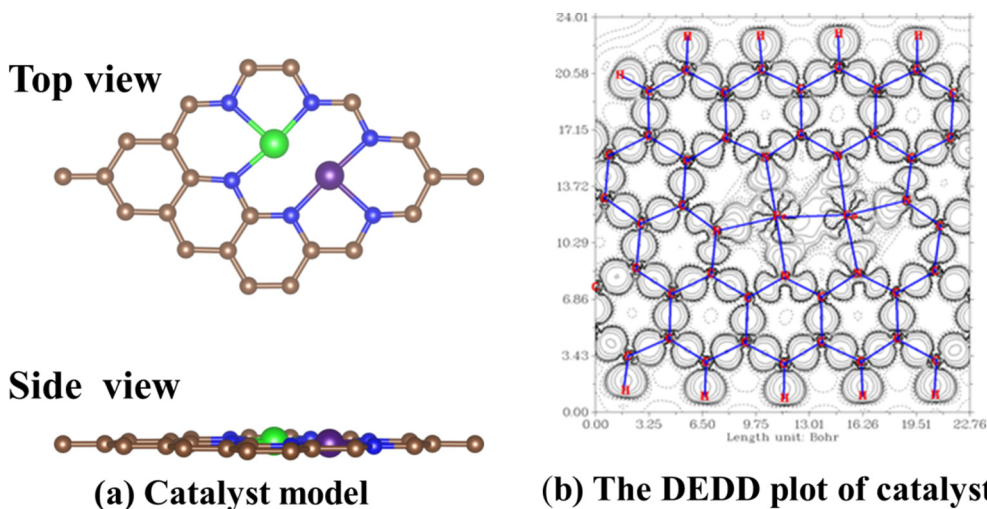


Fig. 1. (Fe,Co)@N-GN model and its DEDD plot.

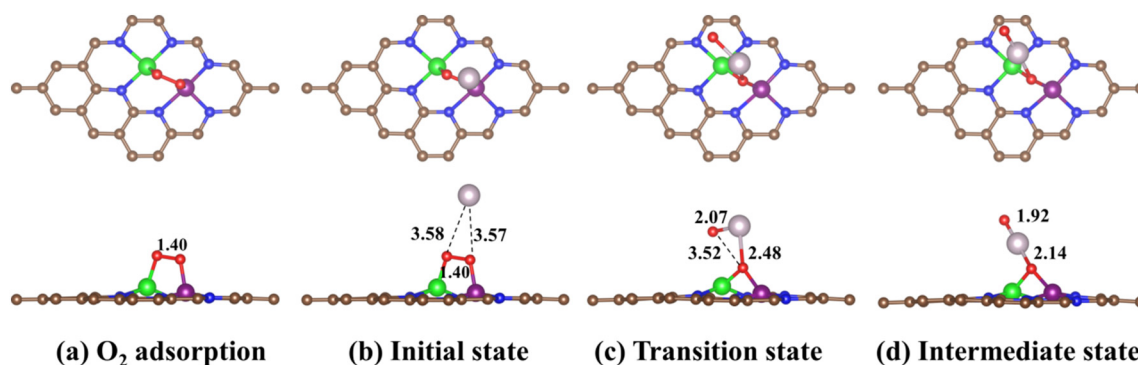


Fig. 3. The formation of O-Hg-O structure.

As shown in Fig. 3, after O_2 adsorption, the Hg^0 molecule would attack the O–O bond to form a structure of O-Hg-O, experiencing an energy barrier about 4.27 eV (from Initial state to Transition state). Though the energy barrier looked very huge, indeed, it has shown greater performance for Hg^0 oxidation, than traditional SCR catalyst in commercial which can oxidize Hg^0 with a high energy barrier about 5.43 eV [53].

3.2.2. HgO desorption and formation of Hg_2O_2 cluster

As shown in Fig. 4, there is a HgO molecule in the structure of O-Hg-O, and therefore after O-Hg-O structure formation, it is likely that the generated HgO molecule would desorb from the surface of catalyst, leaving a single O atom on (Fe,Co)@N-GN surface. In addition, it is noted that in flue gas, the atmosphere is too complicated, and it is also possible that O-Hg-O structure may attract another Hg atom and then form Hg_2O_2 cluster. Taking both possibilities into consideration, we pictured the paths of reaction paths in Fig. 4. In detail, Fig. 4(a) described the process of decomposition of O-Hg-O to generate HgO, and Fig. 4(b) plotted the conformation of Hg_2O_2 cluster.

By theoretical calculation, desorption of HgO from O-Hg-O structure was endothermic with a barrier about 1.85 eV, which was obvious smaller than the energy barrier of oxidation process. Therefore, rate-determining step of Hg^0 catalytic oxidation by (Fe,Co)@N-GN catalyst was oxidation reaction, rather than desorption step, which kept great

consistence with CO oxidation on (Fe,Co)@N-GN catalyst [22]. Moreover, it is worthwhile mention that though there is a residual O atom on the surface of catalyst, it can barely become a large obstacle for next circle of reaction because the residual O atom can easily be consumed by CO and NO molecule in flue gas easily, to produce CO_2 and NO_2 molecule, in the light of previous literature [22]. In addition, the conformation of Hg_2O_2 from O-Hg-O structure was an exothermic process, with heat releasing of 0.02 eV. Afterwards, the generated Hg_2O_2 cluster would desorb from the surface of catalyst, and the desorption energy barrier was about 3.40 eV, and this energy barrier was lower than the energy barrier of Hg^0 oxidation process. Therefore, rate-determining step of formation of Hg_2O_2 cluster by (Fe,Co)/N-GN catalyst was Hg^0 oxidation reaction, rather than desorption step of Hg_2O_2 cluster.

3.3. Gas adsorption on catalyst

3.3.1. Adsorption of SO_3

In order to achieve pollution joint removal in flue gas, five target pollution chemicals were adsorbed on the surface of catalyst, respectively, and the models of pollution gas molecules were adopted from our previous reports [12,34]. The most stable adsorption configurations were selected and then shown in Fig. 5(a)–(e), noted that corresponding adsorption parameters, such as atomic charge, adsorption energy and

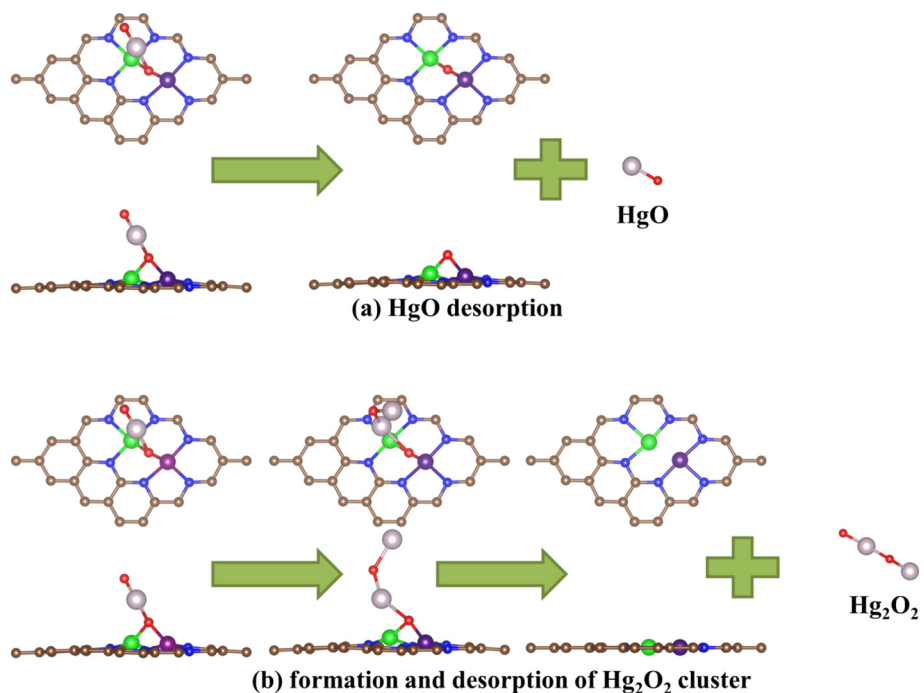


Fig. 4. HgO desorption and formation of Hg_2O_2 cluster.

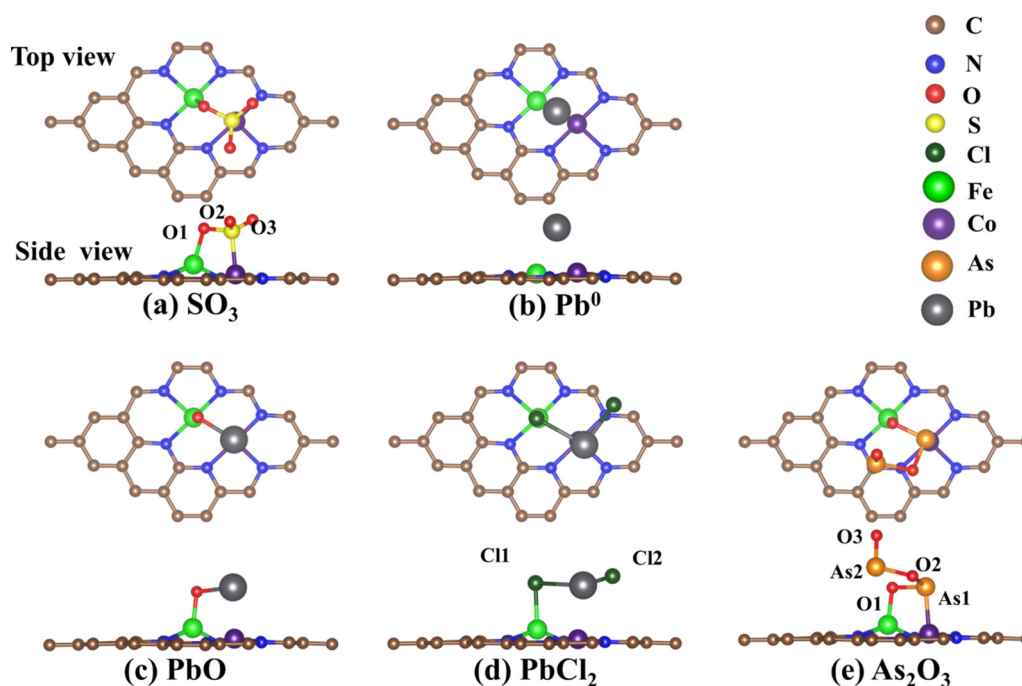


Fig. 5. Adsorption configurations of hazardous gases on catalyst.

Table 2

Bader atomic charge (q), adsorption energy (E_{ads}), and bond length (d) for adsorption configurations.

Gas	None	SO ₃	Pb ⁰	PbO	PbCl ₂	As ₂ O ₃
q_{Fe}/e	0.89	-0.21	0.33	-0.18	-1.06	-0.17
q_{Co}/e	0.61	-0.75	-0.52	-0.53	-0.56	-0.59
$q_{substance}/e$	-1.50	1.90	1.50	1.53	0.19	1.33
E_{ads}/eV	\	-1.83	-2.26	-2.33	-1.31	-1.36
$d_{Fe-Co}/\text{\AA}$	2.19	2.45	2.33	2.45	2.39	2.40
$d_{Fe-O1}/\text{\AA}$	\	1.92	\	1.82	\	1.90
$d_{Co-S}/\text{\AA}$	\	2.18	\	\	\	\
$d_{Fe-Pb}/\text{\AA}$	\	\	2.56	3.07	3.46	\
$d_{Co-Pb}/\text{\AA}$	\	\	2.54	2.57	2.72	\
$d_{O-Pb}/\text{\AA}$	\	\	\	2.14	\	\
$d_{Cl1-Pb}/\text{\AA}$	\	\	\	\	2.73	\
$d_{Cl2-Pb}/\text{\AA}$	\	\	\	\	2.54	\
$d_{Cl1-Fe}/\text{\AA}$	\	\	\	\	2.32	\
$d_{Cl2-Co}/\text{\AA}$	\	\	\	\	4.02	\
$d_{Co-As1}/\text{\AA}$	\	\	\	\	\	2.36
$d_{O1-As1}/\text{\AA}$	\	\	\	\	\	1.84
$d_{O2-As1}/\text{\AA}$	\	\	\	\	\	1.79
$d_{O2-As2}/\text{\AA}$	\	\	\	\	\	1.92
$d_{O3-As2}/\text{\AA}$	\	\	\	\	\	1.64

bond length have been listed in Table 2.

SO₃ molecule was considered to be a soluble gas which can be removed in WFGD, however, about 1%–2% SO₃ gas can be converted to SO₃ colloid with the characteristic of insoluble. Considering the huge amount of fuel consuming and high content of SO_x in flue gas of coal-fired power plants, it is necessary to put the abatement of SO₃ into consideration in the field of pollution integrated removal. Various adsorption positions of SO₃ were considered, and we selected the configurations owning the largest adsorption energy for further investigation, due to its high stability in thermodynamics. From Table 2, the adsorption energy of SO₃ on (Fe,Co)@N-GN catalyst is up to -1.83 eV, demonstrating this adsorption belongs to chemical adsorption, and thus (Fe,Co)@N-GN catalyst has compelling adsorption capacity for SO₃. In addition, according to some literatures of other research, adsorption energy of SO₃ on the surface of single atom iron catalyst based on single vacancy graphene (Fe/SG) was -1.81 eV [34]. Considering Fe/SG has

been considered as an outstanding sorbent in series gases, and (Fe,Co)@N-GN owned stronger adsorption capacity for SO₃, it is reasonable for us to look (Fe,Co)@N-GN as a great sorbent for SO₃.

3.3.2. Adsorption of Pb species (Pb⁰, PbO, and PbCl₂)

The stable adsorption configuration of Pb⁰ on (Fe,Co)@N-GN were shown in Fig. 5(b), and it was observed that the Pb⁰ molecule was attached at the position above active center of catalyst. From Table 2, the adsorption energy of Pb⁰ on (Fe,Co)@N-GN catalyst reached -2.26 eV, suggesting this adsorption belongs to chemical adsorption, and (Fe,Co)@N-GN catalyst has good adsorption capacity for Pb⁰. It is obvious that the adsorption effect of catalyst for Pb⁰ is better than Hg⁰, which may well explained by unfilled 6p orbit of Pb atom. Compared to other research, the E_{ads} of Pb⁰ toward Fe/SG are -1.55 eV [12], which is smaller than the E_{ads} of Pb⁰ toward (Fe,Co)@N-GN, further evidencing (Fe,Co)@N-GN has good adsorption activity for Pb⁰. Besides, the adsorption energy of PbO and PbCl₂ on (Fe,Co)@N-GN catalyst can reach -2.33 eV and -1.31 eV, respectively, and these values indicated (Fe,Co)@N-GN also have good adsorption capacity for main lead species compounds.

3.3.3. Adsorption of As₂O₃

The adsorption of As₂O₃ on (Fe,Co)@N-GN was investigated, and detailed adsorption configuration was shown in Fig. 5(e). Obviously, different from the adsorption of SO₃ and three kinds of Pb species, As₂O₃ molecule experienced a large structural distortion in adsorption process, and this huge change would affect the adsorption energy deeply. According to our calculation, the adsorption energy of As₂O₃ on (Fe,Co)@N-GN was about -1.36 eV, suggesting this adsorption belonged to chemical adsorption as well, similar to SO₃ and Pb species. Therefore, considering (Fe,Co)@N-GN has great adsorption capacity for both SO₃, Pb species, and As₂O₃ molecules, we could think of this catalyst to be a great candidate for simultaneous removal of multiple pollutants in flue gas.

The adsorption order of gases on the surface of (Fe,Co)@N-GN is complicated, but we can observe that it is determined by the presence type of Pb species. Therefore, the adsorption order of Pb⁰, PbCl₂, and PbO is talked about herein. As we know, great activation of gas on the

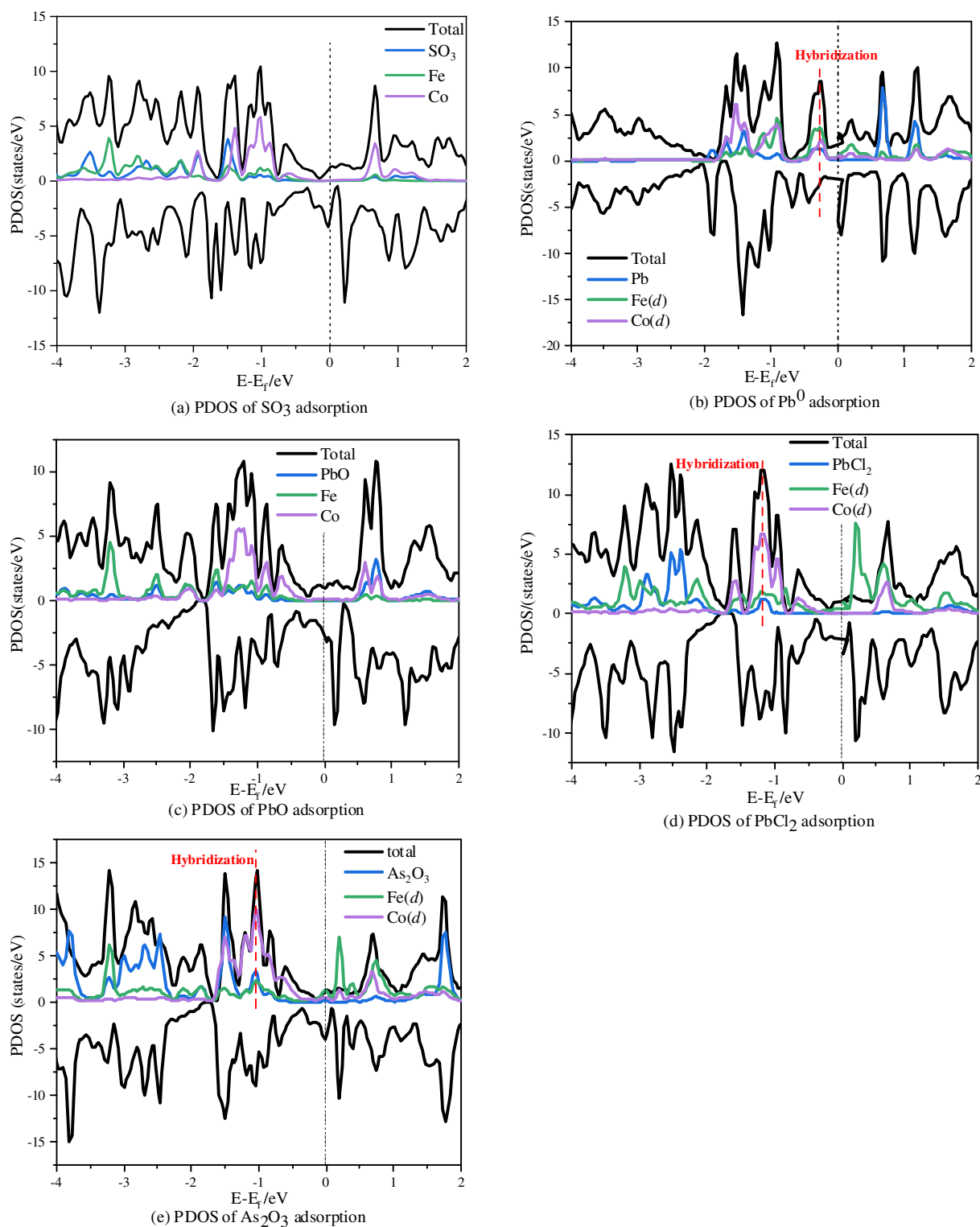


Fig. 6. PDOS of gas adsorption systems.

surface of sorbent is considered to be closely related to adsorption ability. According to previous works of ours [12], the bond length of Pb–O (PbO) and Pb–Cl (PbCl_2) were 1.96 Å and 2.49 Å respectively, and the bond length of Fe–Co of $(\text{Fe,Co})@\text{N-GN}$ was 2.19 Å. Obviously, the bond length of Pb–O is smaller than that of Fe–Co, suggesting there would be great activation of PbO by two metal atoms due to pulling effect. However, the bond length of Pb–Cl is larger than that of Fe–Co. Therefore, compared with Pb^0 , and PbCl_2 , the dual reaction sites give a

fierce pulling effect for PbO , which may contribute to the highest adsorption ability.

3.4. PDOS analysis of pollution gas on catalyst

In order to further understand the adsorption characteristic of pollution gas on $(\text{Fe,Co})@\text{N-GN}$, the PDOS plots were provided to research the role covalent bond played in adsorption, as shown in Fig. 6. First,

the PDOS plot of SO_3 adsorption system was pictured and apparently, no obvious hybridization took place between Fe and Co, as well as SO_3 and sorbent. Hence, the interaction between Fe and Co was weak, and there was no covalent bond between SO_3 molecule and $(\text{Fe,Co})@\text{N-GN}$. In addition, the PDOS of Pb^0 adsorption was calculated to offer a comprehensive insight about Pb^0 adsorption, as shown in Fig. 6(b). Different from SO_3 , there was obvious hybridization among Fe, Co and Pb atoms, which indicated covalent bond made contribution to the high adsorption energy. Similarly, it was easily obtained that no obvious hybridization existed during PbO adsorption, however, hybridization effect induced the interaction between $(\text{Fe,Co})@\text{N-GN}$ and pollution molecules in the adsorption of PbCl_2 and As_2O_3 . So, the mechanism of high adsorption energy about different pollution chemicals on $(\text{Fe,Co})@\text{N-GN}$ was different: For Pb^0 , PbCl_2 , and As_2O_3 , hybridization between gas molecules and catalyst contributed to adsorption greatly, but for SO_3 and PbO , hybridization has no relationship with adsorption energy.

3.5. EDD analysis

Considering electronic transition has been considered to mainly contribute to the formation of interatomic ionic bond, EDD analysis was carried out to further investigate the adsorption interaction of gases on active sites. In detail, the definition of EDD is the charge difference of stable adsorption system (ρ_{ads}) to two isolated system of adsorbent ($\rho_{catalyst}$) and adsorbed gases (ρ_{gas}) on adsorption configurations one by one, and it can be described by the following equation: $EDD = \rho_{ads} - \rho_{gas} - \rho_{catalyst}$ [25].

The EDD images of five hazardous gases on $(\text{Fe,Co})@\text{N-GN}$ catalyst have been plotted in Fig. 7, noted that cyan-blue part represented area losing electron while yellow part mean area gaining electron. In detail, for SO_3 adsorption in Fig. 7(a), there exists obvious electronic transition, suggesting strong interaction between catalyst and SO_3 . In addition, it was captured that plenty of electrons were escaping from S–O1 bond, where bond length was enlarged, suggesting SO_3 molecule was activated by catalyst. It was worth note that the adsorption of SO_3 molecule on catalyst belonged to chemical adsorption, but no covalent bond existed between SO_3 and catalyst by PDOS analysis, so the strong interaction between SO_3 and catalyst should contribute to the ionic

bond due to fierce electronic exchanges. As for Pb^0 , we observed large amounts of electron are focusing on Pb–Fe as well as Pb–Co bond after Pb^0 being adsorbed on catalyst, as shown in Fig. 7(b), indicating strong adsorption energy (-2.26 eV) of Pb^0 on catalyst should contribute to not only the covalent bond, but also the co-effect of ionic bond. Besides, from EDD image of PbO adsorption configuration in Fig. 7(c), the electron mainly distribute on Fe–O bond as well as Co–Pb bond, indicating there were stable adsorption effect on the surface of catalyst. Herein, we found there was no electron concentration between Pb atom and O atom, and the bond length of Pb–O has reach 2.14 Å, from the value of 1.92 Å in its gas state [54], which demonstrated that $(\text{Fe,Co})@\text{N-GN}$ catalyst had outstanding capacity of molecular activation. Fig. 7(d) offered the EDD plot of PbCl_2 adsorption on catalyst, and similar to Fig. 2(a)–(c), we found obvious electronic transfer among whole adsorption system. As for As_2O_3 , its adsorption belonged to dissociation adsorption, and there were obvious electronic acceleration between metal atoms on graphene and pollution gases. In general, there was large amounts of electrons transfer between gas molecules and catalyst, which greatly promoted the adsorption energy of gas on catalyst, and $(\text{Fe,Co})@\text{N-GN}$ catalyst can stretch small gas molecules and destroy shared electrons in gas molecule forcedly. This phenomenon kept great agreement with the previous investigations that $(\text{Fe,Co})@\text{N-GN}$ catalyst showed boosting performance on O_2 adsorption and activation in both experimental and theoretical studies [22,27].

3.6. Thermodynamics analysis

Though adsorption energy analysis based on electronic energy evidenced strong adsorption capacity of $(\text{Fe,Co})@\text{N-GN}$ catalyst on removal of five pollution gases, there was a large confusion on real consequent due to the huge temperature range of flue gas in coal-fired power plants. Considering plenty of reports have argued important effect of temperature on gas adsorption [55,56], and according to the temperature variation of flue gas from boilers outlet to chimney [7], we systematically investigated the changes of adsorption energy from 298.15 K to 1000 K, as plotted in Fig. 8, noted that ΔG represents the adsorption energy based on Gibbs free energy. In detail, the Gibbs free energy of gases and solid surface can be calculated according to these equations:

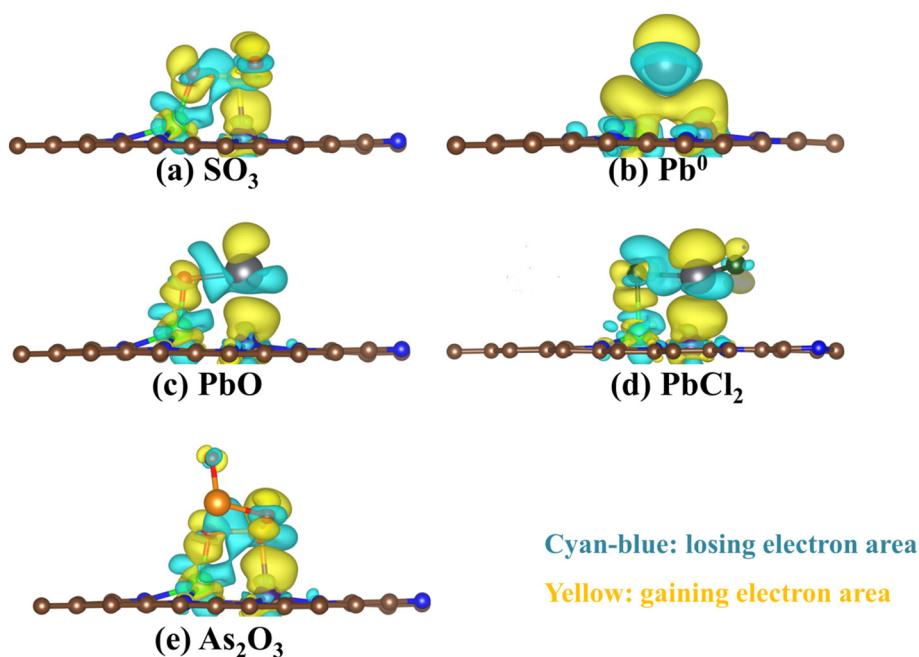


Fig. 7. Electron density difference (EDD) plots of five pollution gases on $(\text{Fe,Co})@\text{N-GN}$ catalyst.

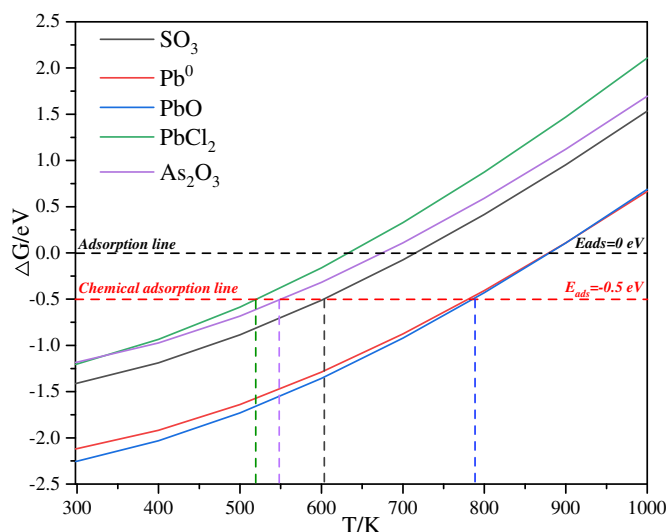


Fig. 8. Adsorption energy variation with different temperatures.

$$G_{\text{gas}} = E_{\text{ele}} + ZPE + RT - TS$$

$$G_{\text{solid}} = E_{\text{ele}} + ZPE - TS$$

where E_{ele} means the electronic energy of chemical, eV; ZPE is the zero point energy correction; R represents the universal gas constant ($8.62 \times 10^{-5} \text{ eV mol}^{-1} \text{ K}^{-1}$); T is the Kelvin temperature, K; S is the entropy of gas or solid chemicals. Thus, the adsorption energy of gases can be obtained according to the following equations:

$$\Delta G_{\text{gas}} = G_{\text{gas-solid}} - G_{\text{gas}} - G_{\text{solid}}$$

In detail, calculation of Gibbs free energy is based on frequency analysis. The vibrational frequency calculations were performed through numerical Hessian calculations with finite displacements of $\pm 0.02 \text{ \AA}$.

From Fig. 8, it was observed that the adoption order of pollution gas was nearly a constant, presented as $\text{PbO} > \text{Pb}^0 > \text{SO}_3 > \text{As}_2\text{O}_3 > \text{PbCl}_2$, and this sequence kept great consistence with the adsorption energy analysis above (see Table 2), suggesting temperature would not change the adsorption order of gases. In addition, it is obviously that the adsorption energy decreases with the raise of temperature, and the adsorption would be always belonging to chemical adsorption while the temperature is lower than 550 K.

Considering in the process of simultaneous removal of multiple pollutants, adsorption process of toxic gases should not be on high temperature condition to avoid oxidation of carbon material catalyst, the compelling performance of (Fe,Co)@N-GN catalyst at low temperature made it a qualified candidate in sorbent selection.

3.7. Competitive adsorption analysis

The removal order of corresponding gases in flue gas is an important issue during simultaneous removal of multiple pollutants. To further investigate the adsorption mechanism of different gases toward (Fe,Co)@N-GN catalyst at the same time, competitive adsorption analysis was performed, using Boltzmann distribution function (B_{df}), which have been widely utilized in researches [57], and it can be calculated by equation as follows:

$$B_{df} = \frac{N_A}{N_B} = \exp\left(-\frac{G(A) - G(B)}{kT}\right)$$

where $G(A)$ and $G(B)$ are on behalf of the Gibbs free energy of gas A and gas B, respectively, eV; k means the value of Boltzmann constant, $8.62 \times 10^{-5} \text{ eV}\cdot\text{K}^{-1}$; T represents the Kelvin temperature of research system, K.

In general, B_{df} pictures the adsorption capacity of different gases toward catalyst, and it is obviously that the bigger value of B_{df} is, the larger will be the possibility for gas A of being adsorbed on sorbent, prior to gas B. The B_{df} makes the competitive adsorption behavior among gas molecules visible and quantitative, therefore offering a great perspective for us to understand gas competitive adsorption at molecule scale. In the light of Fig. 8, the adsorption of PbCl_2 molecule on (Fe,Co)@N-GN catalyst was the weakest, and so we selected adsorption energy of PbCl_2 as a reference amount, that's gas B, to perform calculation work of B_{df} , and the variation of B_{df} value was provided in Fig. 9(a). Competitive analysis showed similar result to the conclusion thermodynamics analysis made on adsorption order of gases, presented as $\text{PbO} > \text{Pb}^0 > \text{SO}_3 > \text{As}_2\text{O}_3 > \text{PbCl}_2$ approximately.

Given the huge volume fraction difference of corresponding gases might affect adsorption order obviously. Based on B_{df} , and taking into consideration of the volume fraction difference of gases in flue gas, we further defined a new descriptor R_T , noted that X_A and X_B represent volume fraction of gas A and gas B.

$$R_T = \exp\left(-\frac{G(A) - G(B)}{kT}\right) \times \frac{X_A}{X_B}$$

R_T was used to further investigate competitive adsorption

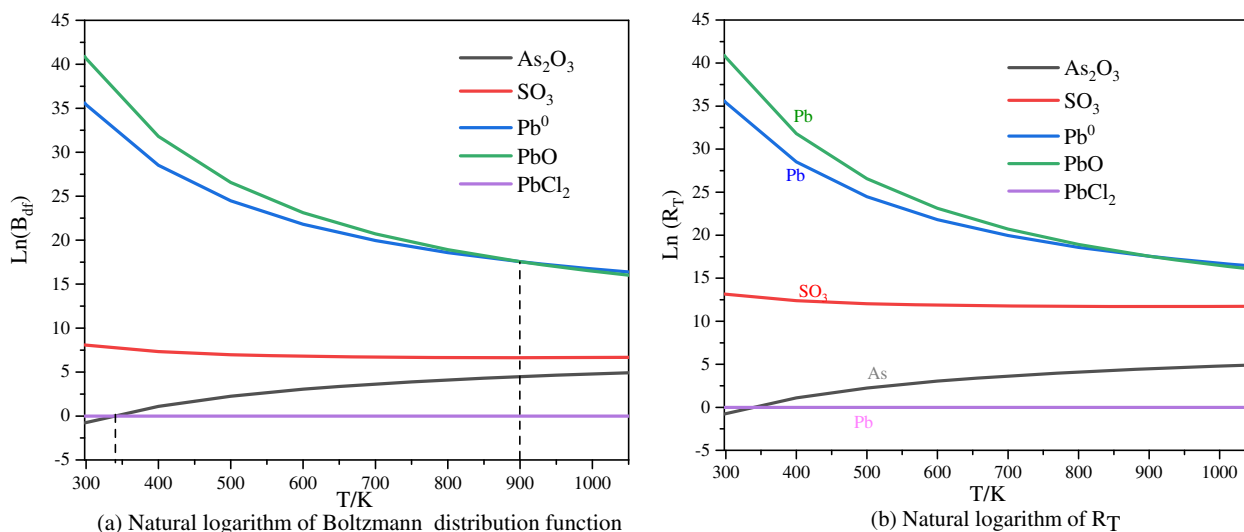


Fig. 9. Competitive adsorption of pollution gases on (Fe,Co)@N-GN.

combining the factors of adsorption energy and gas concentration, and the detailed gas concentration of Pb specie (about 0.05 ppm) and As specie (about 0.05 ppm) was calculated from reports of pollution release from a 350 MW boiler [58,59]. Besides, in the light of large amount of literatures [24,60], 300 ppm–500 ppm was common value of SO₂ volume fraction in flue gas. Besides, oxidation rate of SO₂ in power plants was about 1%–2%, so we thought the concentration of SO₃ was about 8 ppm. Therefore, the R_T was calculated in this work, and has been plotted in Fig. 9(b).

As shown in Fig. 9(b), the adsorption order of gases was not changed compared with the result from B_{df} , even though the possibility of SO₃ being adsorbed became larger than before on the condition that we considered the effect of gas concentration, suggesting the adsorption activity of gas molecule played a more important role, compared to the effect of volume fraction of research gases. In addition, it seemed that the winner of competitive adsorption between SO₃, Pb and As species highly depended on specific forms of Pb species. When Pb species were mainly composed of PbO and Pb⁰, it would be adsorbed by (Fe,Co)@N-GN catalyst firstly, prior to As species and SO₃. However, if Pb species mainly consisted of PbCl₂, it can hardly occupy the reactive sites on catalyst, and therefore it cannot be removed until most of As and SO₃ were solved thoroughly.

4. Conclusions

In order to search qualified catalyst/sorbent for simultaneous removal of multiple pollutants in flue gas, the mechanism of Hg⁰ oxidation, and the adsorption characteristics of SO₃, Pb species and As₂O₃ was research systematically via density functional theory. Deriving from these calculated and results, five conclusions have been acquired as follows:

- (1) (Fe,Co)@N-GN catalyst was stable enough due to huge binding energy of Fe atom and Co on N-doped graphene, and the ionic bond (Fe–N and Co–N) made great contribution to the strong binding energy.
- (2) The energy barrier of Hg⁰ oxidation on the (Fe,Co)@N-GN catalyst was 4.27 eV, which much lower than conventional SCR catalyst, suggesting (Fe,Co)@N-GN was a qualified catalyst for Hg⁰ oxidation.
- (3) Both SO₃, Pb species and As₂O₃ adsorption on (Fe,Co)@N-GN catalyst belonged to chemical adsorption. According to PDOS and EDD analysis, the high adsorption energy of SO₃ and PbO can mainly contribute to large amounts of electron transfer, but the fierce interaction between As₂O₃, Pb⁰, PbCl₂ and catalyst should depend on the combined effect of hybridization and electron transfer.
- (4) Thermodynamics analysis indicated that (Fe,Co)@N-GN was a compelling sorbent for SO₃, Pb species and As₂O₃ chemicals, especially at low temperature.
- (5) Competitive analysis suggested that the adsorption order of pollution gas was determined by adsorption energy, rather than the volume fraction of corresponding gases in flue gas.

Declaration of competing interest

The authors declare no competing financial interest.

Acknowledgement

This work was supported by Beijing Natural Science Foundation (2182066), Natural Science Foundation of Hebei Province (B2018502067), the Fundamental Research Funds for the Central Universities (JB2015RCY03 and 2017XS121) and computational resources from TianHe-2 supercomputer at the Lvliang Supercomputer Center were acknowledged.

References

- [1] Y. Tang, W. Chen, C. Li, L. Pan, X. Dai, D. Ma, Adsorption behavior of Co anchored on graphene sheets toward NO, SO₂, NH₃, CO and HCN molecules, *Appl. Surf. Sci.* 342 (2015) 191–199.
- [2] J. Liu, W. Qu, S.W. Joo, C. Zheng, Effect of SO₂ on mercury binding on carbonaceous surfaces, *Chem. Eng. J.* 184 (2012) 163–167.
- [3] P. Chen, M. Gu, X. Chen, J. Chen, Study of the reaction mechanism of oxygen to heterogeneous reduction of NO by char, *Fuel* 236 (2019) 1213–1225.
- [4] Y. Tang, W. Chen, J. Zhou, H. Chai, Y. Li, Y. Cui, Z. Feng, X. Dai, Mechanistic insight into the selective catalytic oxidation for NO and CO on co-doping graphene sheet: a theoretical study, *Fuel* 253 (2019) 1531–1544.
- [5] J. Dong, Z. Gao, W. Yang, A. Li, X. Ding, Adsorption characteristics of Co-anchored different graphene substrates toward O₂ and NO molecules, *Appl. Surf. Sci.* 480 (2019) 779–791.
- [6] X. Li, Q. Huang, C. Luo, Z. Zhang, Y. Xu, L. Zhang, C. Zheng, Effects of acidic gases and operation parameters on denitrification in oxy-fuel CO₂ compression process, *Fuel* 234 (2018) 1285–1292.
- [7] Z. Gao, X. Liu, A. Li, C. Ma, X. Li, X. Ding, W. Yang, Adsorption behavior of mercuric oxide clusters on activated carbon and the effect of SO₂ on this adsorption: a theoretical investigation, *J. Mol. Model.* 25 (2019).
- [8] J. Lu, Z. Zhou, H. Zhang, Z. Yang, Influenced factors study and evaluation for SO₂/SO₃ conversion rate in SCR process, *Fuel* 245 (2019) 528–533.
- [9] S. Wang, Y. Zhang, Y. Gu, J. Wang, X. Yu, T. Wang, Z. Liu, C.E. Romero, W.-p. Pan, Coupling of bromide and on-line mechanical modified fly ash for mercury removal at a 1000 MW coal-fired power plant, *Fuel* 247 (2019) 179–186.
- [10] Y. Zhang, P. Shang, J. Wang, P. Norris, C.E. Romero, W.-p. Pan, Trace element (Hg, As, Cr, Cd, Pb) distribution and speciation in coal-fired power plants, *Fuel* 208 (2017) 647–654.
- [11] W. Yang, Z. Gao, X. Ding, G. Lv, W. Yan, The adsorption characteristics of mercury species on single atom iron catalysts with different graphene-based substrates, *Appl. Surf. Sci.* 455 (2018) 940–951.
- [12] W. Yang, Z. Gao, X. Liu, X. Ding, W. Yan, The adsorption characteristics of As₂O₃, PbO, PbO and PbCl₂ on single atom iron adsorbent with graphene-based substrates, *Chem. Eng. J.* 361 (2019) 304–313.
- [13] Z. Gao, M. Li, Y. Sun, W. Yang, Effects of oxygen functional complexes on arsenic adsorption over carbonaceous surface, *J. Hazard. Mater.* 360 (2018) 436–444.
- [14] W. Yang, Z. Gao, X. Liu, X. Li, X. Ding, W. Yan, Single-atom iron catalyst with single-vacancy graphene-based substrate as a novel catalyst for NO oxidation: a theoretical study, *Cat. Sci. Technol.* 8 (2018) 4159–4168.
- [15] C.E. Council, China Power Industry Annual Development Report 2018 (in Chinese), (2018).
- [16] Z. Wei, S. Yu, Z. Huang, X. Xiao, M. Tang, B. Li, X. Zhang, Simultaneous removal of elemental mercury and NO by mercury induced thermophilic community in membrane biofilm reactor, *Ecotoxicol. Environ. Saf.* 176 (2019) 170–177.
- [17] S. Cui, R. Hao, D. Fu, Integrated method of non-thermal plasma combined with catalytic oxidation for simultaneous removal of SO₂ and NO, *Fuel* 246 (2019) 365–374.
- [18] J. Liu, Q. Falcoz, D. Gauthier, G. Flamant, C.Z. Zheng, Volatilization behavior of Cd and Zn based on continuous emission measurement of flue gas from laboratory-scale coal combustion, *Chemosphere* 80 (2010) 241–247.
- [19] I. Urriza-Arsuaga, M. Bedoya, G. Orellana, Tailored luminescent sensing of NH₃ in biomethane productions, *Sensors Actuators B Chem.* 292 (2019) 210–216.
- [20] R. Bhuvaneshwari, V. Nagarajan, R. Chandiramouli, Arsenene nanoribbons for sensing NH₃ and PH₃ gas molecules – a first-principles perspective, *Appl. Surf. Sci.* 469 (2019) 173–180.
- [21] X. Cheng, Y. Cheng, Z. Wang, C. Ma, Comparative study of coal based catalysts for NO adsorption and NO reduction by CO, *Fuel* 214 (2018) 230–241.
- [22] Z. Gao, X. Liu, A. Li, X. Li, X. Ding, W. Yang, Bimetallic sites supported on N-doped graphene (Fe, Co)/N-GN) as a new catalyst for NO oxidation: a theoretical investigation, *Mol. Catal.* 470 (2019) 56–66.
- [23] C. Chen, Y. Cao, S. Liu, J. Chen, W. Jia, The catalytic properties of Cu modified attapulgite in NH₃-SCO and NH₃-SCR reactions, *Appl. Surf. Sci.* 480 (2019) 537–547.
- [24] C. Chen, W. Jia, S. Liu, Y. Cao, Simultaneous NO removal and Hg⁰ oxidation over CuO doped V₂O₅-WO₃/TiO₂ catalysts in simulated coal-fired flue gas, *Energy Fuel* 32 (2018) 7025–7034.
- [25] W. Yang, Z. Gao, X. Liu, C. Ma, X. Ding, W. Yan, Directly catalytic reduction of NO without NH₃ by single atom iron catalyst: a DFT calculation, *Fuel* 243 (2019) 262–270.
- [26] Z. Wang, J. Liu, Y. Yang, F. Liu, J. Ding, Heterogeneous reaction mechanism of elemental mercury oxidation by oxygen species over MnO₂ catalyst, *Proc. Combust. Inst.* 37 (2019) 2967–2975.
- [27] J. Wang, Z. Huang, W. Liu, C. Chang, H. Tang, Z. Li, W. Chen, C. Jia, T. Yao, S. Wei, Y. Wu, Y. Li, Design of N-coordinated dual-metal sites: a stable and active Pt-free catalyst for acidic oxygen reduction reaction, *J. Am. Chem. Soc.* 139 (2017) 17281–17284.
- [28] J. Wang, W. Liu, G. Luo, Z. Li, C. Zhao, H. Zhang, M. Zhu, Q. Xu, X. Wang, C. Zhao, Synergistic effect of well-defined dual sites boosting the oxygen reduction reaction, *Energy Environ. Sci.* 11 (2018) 3375–3379.
- [29] J.P. Perdew, K. Burke, M. Ernzerhof, Generalized gradient approximation made simple, *Phys. Rev. Lett.* 77 (1996) 3865.
- [30] G. Kresse, J. Furthmüller, Efficiency of ab-initio total energy calculations for metals and semiconductors using a plane-wave basis set, *Comput. Mater. Sci.* 6 (1996) 15–50.

- [31] G. Kresse, J. Furthmüller, Efficient iterative schemes for ab initio total-energy calculations using a plane-wave basis set, *Phys. Rev. B* 54 (1996) 11169.
- [32] Z. Gao, A. Li, X. Liu, C. Ma, X. Li, W. Yang, X. Ding, Density functional study of the adsorption of NO on Ni ($n = 1, 2, 3$ and 4) clusters doped functionalized graphene support, *Appl. Surf. Sci.* 481 (2019) 940–950.
- [33] Z.Y. Gao, W.J. Yang, X.L. Ding, G. Lv, W.P. Yan, Support effects on adsorption and catalytic activation of O₂ in single atom iron catalysts with graphene-based substrates, *Phys. Chem. Chem. Phys.* 20 (2018) 7333–7341.
- [34] Z. Gao, W. Yang, X. Ding, G. Lv, W. Yan, Support effects in single atom iron catalysts on adsorption characteristics of toxic gases (NO₂, NH₃, SO₃ and H₂S), *Appl. Surf. Sci.* 436 (2018) 585–595.
- [35] S. Yang, G. Lei, H. Xu, B. Xu, H. Li, Z. Lan, Z. Wang, H. Gu, A DFT study of CO adsorption on the pristine, defective, In-doped and Sb-doped graphene and the effect of applied electric field, *Appl. Surf. Sci.* 480 (2019) 205–211.
- [36] H. Li, K. Shin, G. Henkelman, Effects of ensembles, ligand, and strain on adsorbate binding to alloy surfaces, *J. Chem. Phys.* 149 (2018) 174705.
- [37] S. Grimme, J. Antony, S. Ehrlich, H. Krieg, A consistent and accurate ab initio parametrization of density functional dispersion correction (DFT-D) for the 94 elements H-Pu, *J. Chem. Phys.* 132 (2010) 154104.
- [38] D. Cortés-Arriagada, N. Villegas-Escobar, A DFT analysis of the adsorption of nitrogen oxides on Fe-doped graphene, and the electric field induced desorption, *Appl. Surf. Sci.* 420 (2017) 446–455.
- [39] G. Henkelman, B.P. Uberuaga, H. Jónsson, A climbing image nudged elastic band method for finding saddle points and minimum energy paths, *J. Chem. Phys.* 113 (2000) 9901–9904.
- [40] G. Henkelman, H. Jónsson, Improved tangent estimate in the nudged elastic band method for finding minimum energy paths and saddle points, *J. Chem. Phys.* 113 (2000) 9978–9985.
- [41] S. Impeng, A. Junkaew, P. Maitarad, N. Kungwan, D. Zhang, L. Shi, S. Namuangruk, A MnN₄ moiety embedded graphene as a magnetic gas sensor for CO detection: a first principle study, *Appl. Surf. Sci.* 473 (2019) 820–827.
- [42] C. Wu, I.D. Gates, Methane activation by a single iron atom supported on graphene: impact of substrates, *Mol. Catal.* 469 (2019) 40–47.
- [43] Z. Gao, W. Yang, Effects of CO/CO₂/NO on elemental lead adsorption on carbonaceous surfaces, *J. Mol. Model.* 22 (2016) 166.
- [44] E. Olson, J. Laumb, S. Benson, G. Dunham, R. Sharma, B. Mibeck, S. Miller, M. Holmes, J. Pavlish, An improved model for flue gas–mercury interactions on activated carbons, *Proceedings of the Combined Power Plant Air Pollutant Control Mega Symposium*, 2003, pp. 19–22.
- [45] H. Zhang, Y. Tang, Y. Ma, D. Ma, M. Zhao, X. Dai, Modulating the gas sensing properties of nitrogen coordinated dopants in graphene sheets: a first-principles study, *Appl. Surf. Sci.* 427 (2018) 376–386.
- [46] P. Janthon, S.M. Kozlov, F. Vines, J. Limtrakul, F. Illas, Establishing the accuracy of broadly used density functionals in describing bulk properties of transition metals, *J. Chem. Theory Comput.* 9 (2013) 1631–1640.
- [47] D. Deng, K.S. Novoselov, Q. Fu, N. Zheng, Z. Tian, X. Bao, Catalysis with two-dimensional materials and their heterostructures, *Nat. Nanotechnol.* 11 (2016) 218–230.
- [48] C. Tabtimasai, T. Sontua, T. Motongsri, B. Wannoo, A DFT study of H₂ CO and HCN adsorptions on 3d, 4d, and 5d transition metal-doped graphene nanosheets, *Struct. Chem.* 29 (2018) 147–157.
- [49] B. Wannoo, C. Tabtimasai, A DFT investigation of CO adsorption on VIIIIB transition metal-doped graphene sheets, *Superlattice. Microst.* 67 (2014) 110–117.
- [50] S. Liang, C. Hao, Y. Shi, The power of single-atom catalysis, *ChemCatChem* 7 (2015) 2559–2567.
- [51] T. Lu, F. Chen, Multiwfn: a multifunctional wavefunction analyzer, *J. Comput. Chem.* 33 (2012) 580–592.
- [52] Y. Gao, Z. Zhang, J. Wu, L. Duan, A. Umar, L. Sun, Z. Guo, Q. Wang, A critical review on the heterogeneous catalytic oxidation of elemental mercury in flue gases, *Environ. Sci. Technol.* 47 (2013) 10813–10823.
- [53] Y. Gao, Z. Li, Y. Hao, Effect of M-doped (M = Cr, Fe, Co, and Nb) V₂O₅/TiO₂ (001) on mercury oxidation: the insights from DFT calculation, *J. Phys. Chem. C* 121 (2017) 27963–27975.
- [54] M. Benavides-Garcia, K. Balasubramanian, Bond energies, ionization potentials, and the singlet–triplet energy separations of SnCl₂, SnBr₂, SnI₂, PbCl₂, PbBr₂, PbI₂, and their positive ions, *J. Chem. Phys.* 100 (1994) 2821–2830.
- [55] X. Tian, J. Min, T. Wang, Coverage dependent CO adsorption manners on seven MoP surfaces with DFT based thermodynamics method, *Appl. Surf. Sci.* 480 (2019) 172–176.
- [56] Y. Ihm, C. Park, J. Jakowski, J.R. Morris, J.H. Shim, Y.-H. Kim, B.G. Sumpter, M. Yoon, Assessing the predictive power of density functional theory in finite-temperature hydrogen adsorption/desorption thermodynamics, *J. Phys. Chem. C* 122 (2018) 26189–26195.
- [57] Z. Gao, Y. Sun, M. Li, W. Yang, X. Ding, Adsorption sensitivity of Fe decorated different graphene supports toward toxic gas molecules (CO and NO), *Appl. Surf. Sci.* 456 (2018) 351–359.
- [58] S. Zhao, Y. Duan, L. Chen, Y. Li, T. Yao, S. Liu, M. Liu, J. Lu, Study on emission of hazardous trace elements in a 350 MW coal-fired power plant. Part 2. Arsenic, chromium, barium, manganese, lead, *Environ. Pollut.* 226 (2017) 404–411.
- [59] S. Zhao, Y. Duan, L. Chen, Y. Li, T. Yao, S. Liu, M. Liu, J. Lu, Study on emission of hazardous trace elements in a 350 MW coal-fired power plant. Part 1. Mercury, *Environ. Pollut.* 229 (2017) 863–870.
- [60] H. Yi, C. Ma, X. Tang, S. Zhao, K. Yang, Z. Sani, L. Song, X. Zhang, W. Han, Synthesis of MgO@CeO₂-MnOx core shell structural adsorbent and its application in reducing the competitive adsorption of SO₂ and NOx in coal-fired flue gas, *Chem. Eng. J.* 372 (2019) 129–140.